Evolution, 2023, **77(6)**, 1277–1288
https://doi.org/10.1093/evolut/qpad056
Advance access publication 30 March 2023
Original Article

How to tuna fish: constraint, convergence, and integration in the neurocranium of pelagiarian fishes

Andrew Knapp[1], Gizéh Rangel-de Lázaro[1,2], Matt Friedman[3], Zerina Johanson[1], Kory M. Evans[4], Sam Giles[5], Hermione T. Beckett[6], Anjali Goswami[1]

[1]Department of Science, Natural History Museum, London, United Kingdom
[2]School of Museum Studies, University of Leicester, Leicester, United Kingdom
[3]Department of Earth and Environmental Sciences, University of Michigan, Ann Arbor, MI, United States
[4]Department of Biosciences, Rice University, Houston, TX, United States
[5]Department of Geography, Earth and Environmental Sciences, University of Birmingham, Birmingham, United Kingdom
[6]Department of Biology, King's High School for Girls, Warwick, United Kingdom

Corresponding author: Department of Science, Natural History Museum, Cromwell Road, London, SW7 5BD, United Kingdom. Email: a.knapp@nhm.ac.uk

Abstract

Morphological evolution of the vertebrate skull has been explored across a wide range of tetrapod clades using geometric morphometrics, but the application of these methods to teleost fishes, accounting for roughly half of all vertebrate species, has been limited. Here we present the results of a study investigating 3D morphological evolution of the neurocranium across 114 species of Pelagiaria, a diverse clade of open-ocean teleost fishes that includes tuna and mackerel. Despite showing high shape disparity overall, taxa from all families fall into three distinct morphological clusters. Convergence in shape within clusters is high, and phylogenetic signal in shape data is significant but low. Neurocranium shape is significantly correlated with body elongation and significantly but weakly correlated with size. Diet and habitat depth are weakly correlated with shape, and nonsignificant after accounting for phylogeny. Evolutionary integration in the neurocranium is high, suggesting that convergence in skull shape and the evolution of extreme morphologies are associated with the correlated evolution of neurocranial elements. These results suggest that shape evolution in the pelagiarian neurocranium reflects the extremes in elongation found in body shape but is constrained along relatively few axes of variation, resulting in repeated evolution toward a restricted range of morphologies.

Keywords: geometric morphometrics, teleost, Pelagiaria, morphological evolution

Introduction

The open ocean is the largest single habitat on Earth. In contrast to structurally complex biodiverse settings like coral reefs (Rabosky *et al.*, 2018; Roberts *et al.*, 2002), it might seem environmentally homogenous, but the wide range of light levels, temperatures, currents, and food availability creates a surprising diversity of ecological niches that may drive adaptation. Most research on the phenotypic evolution of marine fishes focuses on clades (Evans *et al.*, 2022; Larouche *et al.*, 2022) or assemblages (Claverie & Wainwright, 2014) principally associated with shallow-water, coastal settings, often in proximity to reefs. However, recent surveys of fishes across marine habitats reveal that some settings are unexpected hotspots of phenotypic evolution (Friedman *et al.*, 2019; Martinez *et al.*, 2021). This previous work largely focuses on patterns of morphological diversity or rates of evolutionary change, with an emphasis on extrinsic factors that may contribute to elevated phenotypic variety (see Collar *et al.*, 2022). Intrinsic aspects potentially facilitating anatomical divergence have, by contrast, been little explored for these groups.

Modularity is an aspect of organismal structure often implicated in mediating patterns of evolutionary diversification. Modularity refers to trait complexes (i.e., "modules") with high internal integration while showing much lower integration between trait complexes (Zelditch & Goswami, 2021). The ability of sets of traits to covary in this way is thought to permit quasi-independent responses to selection. This in turn may result in mosaic evolution over macroevolutionary timescales because modules are able to independently adapt to localized selective pressures and diverge in evolutionary patterns accordingly. Conversely, higher integration between modules is expected to evolve when there is selective pressure for these modules to covary more strongly. Although highly modular structures may be able to evolve a wider range of morphologies, higher levels of integration are thought to promote the evolution of extreme morphologies by partitioning variance along fewer preferred trajectories (Goswami *et al.*, 2014; Hedrick *et al.*, 2020). Modularity has also been hypothesized to increase through evolutionary time to circumvent developmental constraints (Goswami *et al.*, 2014; Wagner & Altenberg, 1996). While phenotypic integration, which focuses on the species level and below, reflects the processes causing integration, and thus driving evolutionary patterns, evolutionary integration, which we focus on here, reflects the outcome of those causal processes, which can underlie the correlated evolution of traits (Zelditch & Goswami, 2021).

Received December 20, 2022; revisions received March 10, 2023; accepted March 29, 2023

Many recent studies of both phenotypic and evolutionary integration and modularity have largely focused on tetrapod clades (Arbour *et al.*, 2021; Bardua *et al.*, 2019; Bibi & Tyler, 2022; Felice & Goswami, 2017; Felice *et al.*, 2019; Goswami & Polly, 2010; Hanot *et al.*, 2021; Randau & Goswami, 2018; Rhoda *et al.*, 2021; Watanabe *et al.*, 2019), but despite accounting for roughly 50% of the 60,000 named species of vertebrates, teleost fishes have received comparatively little attention, with most comparative studies in this clade focusing on modularity in body shape (Black & Armbruster, 2022; Burns *et al.*, 2023; Denton & Adams, 2015; Larouche *et al.*, 2018), feeding apparatus (Collar *et al.*, 2014; Conith & Albertson, 2021; Conith *et al.*, 2020; Jamniczky *et al.*, 2014), or unique or highly-specialized morphologies (Evans *et al.*, 2017a, b; Evans *et al.*, 2019, 2021; but see Evans *et al.*, 2022; Larouche *et al.*, 2022; Lehoux & Cloutier, 2015). The teleost skull comprises a large number of kinetic and akinetic elements that can be broadly divided into two regions: the rigidly associated neurocranium, including the skull roof, braincase, and upper margin of the orbit (Nelson, 2006), and the splanchnocranium, representing the kinetic elements of the upper and lower jaws, suspensorium, operculum, and other mouth and gill parts (Gregory, 1932). The relatively large number of skull elements in modern teleosts suggests that the structure may be highly modular, even in rigid, fused regions such as the neurocranium (Evans *et al.*, 2017b, 2021), though brain development is known to influence neurocranial integration in vertebrates because it signals the development of overlying tissues and spans a number of enclosing elements (Evans *et al.*, 2017a; Hu & Marcucio, 2009; Northcutt & Kaas, 1995). Similarly, the tetrapod skull has been shown to be highly modular despite the loss or complete fusion of a number of skull elements through evolutionary history (Bardua *et al.*, 2019; Fabre *et al.*, 2020; Felice & Goswami, 2017; Felice *et al.*, 2019; Goswami *et al.*, 2014). The developmental and evolutionary decoupling of the kinetic splanchnocranium may have allowed teleosts to exploit a wide range of niches by enabling the evolution of diverse feeding strategies (Larouche *et al.*, 2022), although the oral and pharyngeal jaws of many teleost taxa have been shown to be highly integrated themselves (Conith & Albertson, 2021; Conith *et al.*, 2020; Jamniczky *et al.*, 2014; Larouche *et al.*, 2022). Understanding patterns of integration is therefore an important step in understanding the evolution of this complex structure in teleosts in context with better-understood tetrapod groups.

Teleosts are separated from tetrapods by some 425 million years of evolution and so establishing direct homology between skull elements of these groups is difficult (Schultze *et al.*, 2008; Thomson, 1993). Comparison is further complicated by the differences in the number and type of skull elements and high kinesis of the mouth and opercular regions of teleosts. The neurocranium, a single, akinetic structure, forms a logical basis for assessing integration and evolution of the teleost skull as an analog to the rigid tetrapod skull. The neurocranium has four main roles: it protects and supports the brain and cranial sensory organs, provides structure and shape to the skull and anterior body, acts as a rigid anchor to the kinetic splanchnocranial elements, and anchors the spinal column and associated axial musculature important in modulating feeding and respiration (Camp *et al.*, 2015; Gregory, 1932). In contrast to the teleost skull, the tetrapod skull is largely akinetic, incorporating elements involved in feeding (e.g., maxilla, premaxilla) with the neurocranium into a single, rigid structure. Consequently, when treated as a single unit, the tetrapod skull performs additional functions to the teleost neurocranium. Nonetheless, the main roles of the teleost neurocranium, as outlined above, also apply to the cranial region of the tetrapod skull, and this can provide a basis for comparisons between the two groups.

Geometric morphometrics provides a means to capture and statistically quantify form across a clade in great detail, allowing for the testing of evolutionary hypotheses in a phylogenetic framework (Goswami *et al.*, 2019). The taxonomic diversity of teleosts poses a challenge to any comprehensive attempt to quantify biological form using this approach because of the difficulty of assembling a representative sample. By focusing on a single clade, it is possible to sample the majority of shape variation and place it in a phylogenetic context, without the need for sampling potentially thousands of individuals. The clade Pelagiaria comprises 286 species of open-ocean fishes in 75 genera and 15 families, including well-known taxa such as tuna (*Thunnus*) and mackerel (*Scomber*) (Arcila *et al.*, 2021; Friedman *et al.*, 2019; Miya *et al.*, 2013). It was recognized as monophyletic only through the application of molecular systematic (Bentacur-R *et al.*, 2017; Hughes *et al.*, 2018); traditional morphological classifications dispersed its members between at least six suborders thought to be distantly related to one another (Pastana *et al.*, 2021). The oldest fossil pelagiarians are Paleocene in age and paleontologically calibrated molecular phylogenies indicate an origin around the Cretaceous–Paleogene (K/Pg) boundary (Friedman *et al.*, 2019). Fossil evidence shows that familiar modern body plans for at least some of these families had become established no later than the early Eocene (ca. 56 Ma; Beckett and Friedman, 2016; Beckett *et al.*, 2018a, b; Monsch & Bannikov, 2011), and these distinctive morphologies may have arisen in as little as 5–7 million years (Friedman *et al.*, 2019), suggesting an early burst model of morphological evolution may be supported for this clade. The K/Pg extinction was selected against predatory marine fishes (Friedman, 2009), suggesting that some pelagiarian lineages exploited these vacated ecological roles in the early Cenozoic. Consequently, this group shows remarkable ecologically and morphologically diversity for its size, with body elongation spanning extremes of the body shape continuum of teleosts, from deep-bodied butterfishes (Stromateidae) to highly elongate scabbardfishes (Trichiuridae) (Collar *et al.*, 2022; Friedman *et al.*, 2019; Friedman *et al.*, 2021). Given the importance of the skull in shaping the anterior body and its role in housing sensory organs and the feeding apparatus, we expect the morphological and ecological diversity of Pelagiaria to be reflected in skull morphology. The relatively small number of taxa and well-resolved phylogeny allow us to conduct a thorough analysis of morphological evolution across the clade.

In this study, we conduct a comprehensive analysis of the pelagiarian neurocranium, using 3D geometric morphometrics to determine patterns of morphological disparity, integration, and evolutionary change across the clade.

Methods

Data collection, imaging, and landmarking

X-ray micro-computed tomography and computed tomography (for larger specimens) were used to create high-definition 3D models of the skulls of spirit-preserved pelagiarian

specimens. One specimen per species of all specimens available to us were scanned, totaling 114 species. These specimens represent 14 of 16 pelagiarian families and 63 of 75 genera (Figure 1; Supplementary Table S1). The specimens analyzed came from repositories at the Natural History Museum (United Kingdom), University of Michigan Museum of Zoology (United States), Field Museum of Natural History (United States), Berlin Zoological Museum (Germany), National Museum of Natural History (France), American Museum of Natural History (United States), Australian Museum (Australia), Yale Peabody Museum (United States), the Natural History Museum of Denmark (Denmark), and Natural History Museums of Los Angeles County (United States).

Specimens were scanned with pixel size and slice thickness ranging between 0.01 and 0.5 mm, and an average set of 1,657 projections for each individual. The digitized cranial bones were segmented and prepared in Materialise Mimics 21.0 (Materialise, 2015) and Geomagic Wrap (3D Systems, 2017). The neurocranium of each specimen was segmented out and exported as a ~1 million polygon mesh ASCII PLY file.

A landmark scheme was devised to capture as much surface morphology as possible, with 99 anatomical (Bookstein Type I) landmarks to capture homologous points and 102 semilandmark curves, totaling 1,063 semilandmarks, to describe sutures and edges (see supplementary information for details). All landmarks and curves were applied with Stratovan Checkpoint (v. 2020.10.13.0859) on the left side of the neurocranium only (Supplementary Figure S1). Landmarks were exported to R and curves were resampled to standardize the number of semilandmarks, then slid to minimize bending energy. Landmarks were reflected across the midline to improve alignment accuracy (Cardini, 2016). A generalized Procrustes alignment (Rohlf & Slice, 1990) was performed on this set of landmarks (original and reflected), before removing the latter to reduce redundant dimensionality. All subsequent analyses were performed on the aligned original landmarks.

Ecological data

Following Friedman *et al.* (2019), additional information was collected for each taxon. Lateral body elongation was calculated as fineness ratio (standard length/body depth) using the measurement protocol outlined in Claverie & Wainwright (2014). With this method, a circular body has a value of 1 and an elongated body has a value of >>1 (Supplementary Table S1). Following Martinez *et al.* (2021), each species was assigned to one of three depth zones. These categories are follows: *Shallow*, equivalent to the epipelagic zone (0–200 m, n = 44); *Intermediate*, equivalent to the mesopelagic zone (200–1,000 m, n = 51); and *Deep*, equivalent to the aphotic bathypelagic and abyssopelagic zones (>1,000 m, n = 17; Supplementary Table S1). Depth information was gathered from Fishbase (Froese & Pauly, 2022) for all species, based on documented observations. Diet data were binned categorically as large evasive prey (e.g., fishes and squid), gelatinous

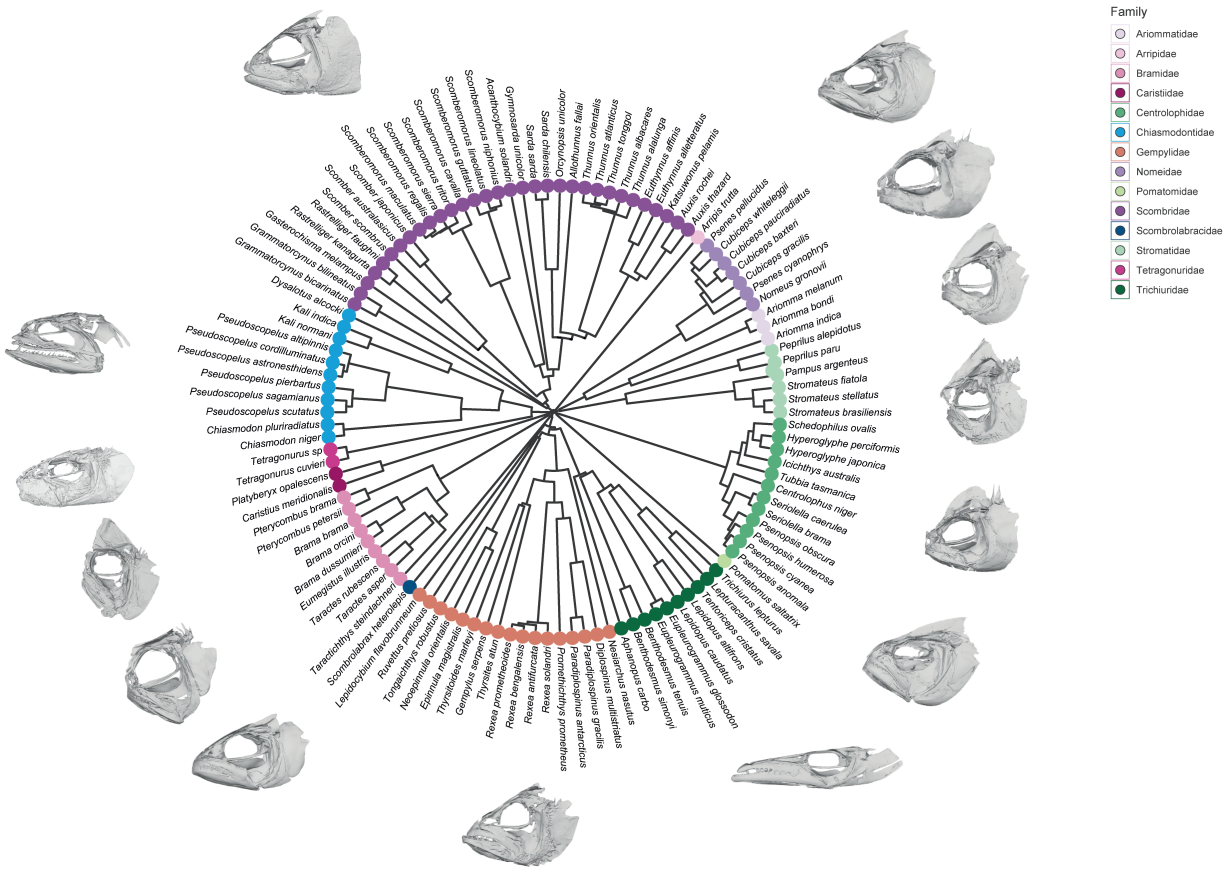

Figure 1. Phylogeny of 114 Pelagiaria species used in this study. Species are colored according to family. Representative whole-skull meshes are shown for each family. See supplementary Table S1 for specimen details.

zooplankton (e.g., jellyfishes, salps), and smaller zooplankton, based on the method used by Friedman *et al.* (2019), with additional data gathered from Fishbase (Froese & Pauly, 2022; Supplementary Table S1).

Phylogeny

We adapted a dated phylogeny for our data set using results from Friedman *et al.* (2019; Figure 1). Additional taxa were added to this phylogeny based on the topology of the concatenation analysis of Arcila *et al.* (2021) and smaller-scale phylogenetic studies by Miya *et al.* (2013), Beckett *et al.* (2018a, b), and Jeena *et al.* (2022) (see Supplementary Table S1 for details). These additional taxa were added first by substituting examples of single, congeneric taxa where possible or by grafting to the Friedman *et al.* phylogeny. Because the majority of additional taxa were nested within known, time-scaled clades, new nodes were time-scaled by arbitrarily placing them 50% along the relevant branch. Where new taxa were placed outside known clades, nodes were set to match the length of the subsequent branch within the time-scaled clade. The exceptions to this were the two taxa of estimated positions, *Orcynopsis unicolor*, which was placed 50% along the branch subtending *Sarda* but within Scombridae, and *Nomeus gronovii*, which was placed 66% along the branch subtending Nomeidae. Friedman *et al.* (2019) and Arcila *et al.* (2021) both support the monophyly of all pelagiarian families except "Gempylidae," with *Lepidocybium flavobrunneum*, traditionally a member of Gempylidae, found to be an outgroup to Gempylidae/Trichiuridae in both. There are some differences in interfamilial relationships between the two studies, namely the placement of Scombridae as a sister group to Tetragonuridae/Chiasmodontidae in Friedman *et al.*, contrasting with Arcila *et al.*, where it is a sister group to clades "A" (Stromateidae/Ariommatidae/Nomeidae), "D" (Caristiidae/Bramidae), and "B" (Gempylidae/Trichiuridae). Additionally, the monotypic families Icosteidae (not included in our study) and Pomatomidae are placed in different positions in the two studies. For consistency, and because it is time-scaled, we used the interfamilial topology of Friedman *et al.* (2019).

Shape analysis

A principal components analysis (PCA) was performed on the Procrustes-aligned landmark data. Major axes of shape variation were visualized with projected neurocranium shapes, created by warping the mean shape to maximum and minimum PC scores using the "tps3d" function in the R package *Morpho* (R Core Team, 2013; Schlager, 2017). All subsequent analyses were performed in R unless otherwise stated.

Allometry was quantified by regressing Procrustes shape data against centroid size using the "procD.lm" function in *geomorph* (Adams & Otárola-Castillo, 2013). We further quantified allometry in cranial shape after accounting for phylogenetic effects with the "procD.pgls" function in *geomorph*. Phylogenetic signal in shape data was calculated for the whole neurocranium and individual modules using a multivariate adaptation of the *K* statistic, K_{mult}, implemented with the function "physignal" in *geomorph* (Adams & Otárola-Castillo, 2013).

To assess morphological convergence in neurocranium shape, a *k*-means cluster analysis was used to identify major clusters within the shape space with the "kmeans" function in R, using the first 35 PC scores (accounting for 95% of total shape disparity) (Tibshirani *et al.*, 2001). Mean shape was calculated for each cluster using the "mshape" function in *geomorph*, and these shapes were visualized by warping a neurocranium mesh using the "tps3d" function in the R package *Morpho* (Schlager, 2017). Morphological convergence within clusters was quantified with the distance-based measure, C, developed by Stayton (2015), an approach that measures the average phenotypic convergence across a group within phylomorphospace. Results were compared with a set of 100 simulations under a Brownian motion (BM) null model of evolution to provide a significant value for each cluster, using the first 35 principal components, accounting for a cumulative 95% of total shape disparity, and implemented with the "convratsig" function in the R package *convevol* (Stayton, 2015).

Modularity analyses

A total of 9 hypotheses of modularity, ranging from a two-module structure to a 16-module structure, were developed to encompass a range of developmental, functional, and regional associations of neurocranial elements (see Supplementary Material for details). Each modularity hypothesis was tested with a covariance ratio (CR) analysis using the *geomorph* functions "modularity.test," on raw shape data, and "phylo.modularity," to account for phylogenetic nonindependence (Adams, 2016). The "compare.CR" function in *geomorph* (Adams & Otárola-Castillo, 2013) was then used to assess the best-supported hypothesis for both raw and phylogenetically informed sets of CR analyses.

Body shape and ecological data

The correlation of fineness ratio, depth, and diet with neurocranium shape was separately assessed with a multivariate regression (for fineness ratio) and a MANOVA (for depth and diet) on the Procrustes shape data, using shape as the dependent variable for each category. These analyses were performed with the R package *geomorph* (Adams & Otárola-Castillo, 2013). The raw shape data were assessed with the "procD.lm" function, and the "procD.pgls" function was used to account for phylogenetic distance.

Martinez *et al.* (2021) found that body shape disparity varied significantly with depth in oceanic teleosts, with deep-sea species showing twice the disparity of shallow-water taxa. To test whether this was the case in Pelagiaria, we performed pairwise comparisons of shape disparity with depth on our data set using the function "morphol.disparity" in *geomorph* (Adams & Otárola-Castillo, 2013).

Evolutionary modeling

We used BayesTraitsV3 (Meade & Pagel, 2014) to estimate evolutionary rates of the entire neurocranium, using the scores of phylogenetic PCs that combined account for >95% of total shape variation. We tested 10 alternative models: fixed and variable rate Brownian motion and Ornstein-Uhlenbeck (OU), with δ, κ, and λ tree transformations. The best-supported evolutionary model was determined with Bayes Factor in the R package *BTprocessR* (Ferguson-Gow, 2021). This process was repeated for each individual module, with globally and locally aligned landmark subsets. Evolutionary rate (σ^2_{mult}) was compared for each module, both globally and locally aligned, using the *geomorph* function "compare.multi.evol.rates" (Adams & Otárola-Castillo, 2013).

Results

Cranial variation

The results of the PCA for the first 3 PCs are shown in Figure 2. PC1 accounts for nearly half of the shape disparity in the neurocranium (46.1%; Supplementary Figure S2). It represents a general transition from an elongate neurocranium typical of Gempylidae and Trichiuridae at negative values, primarily driven by telescoping of the anterior neurocranium, to the short, deep neurocranium of Stromateidae and Bramidae at positive values, with foreshortened anterior

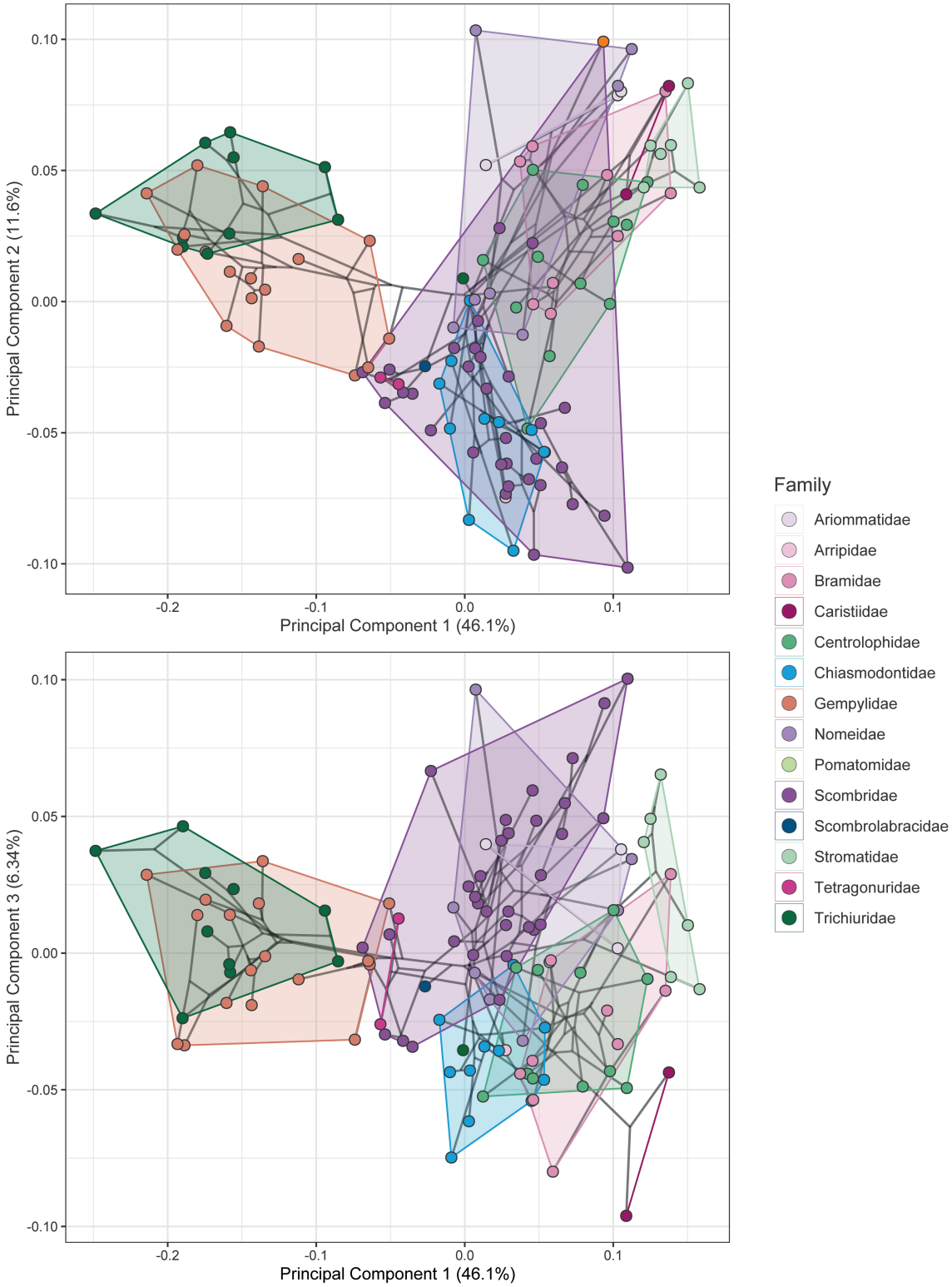

Figure 2. Phylomorphospace of 114 genera of Pelagiaria. Shown are PCs 1 and 2 (top) and PCs 1 and 3 (bottom). First three PCs cumulatively account for ~64% of the total shape disparity. Specimens are colored according to family, with colored convex hulls bounding the morphospace ranges of each family. Projected shapes for extreme PC scores are shown as warped meshes as L: left lateral and D: dorsal view for each PC axis.

neurocranium and typically a tall supraoccipital crest. PC2 accounts for 11.6% of total shape disparity and indicates a transition from a wide, dorsoventrally compressed neurocranium with elongate ethmoid, frontal and lateral ethmoid regions at negative PC scores to a laterally compressed, tall neurocranium with large supraoccipital crest and shortened ethmoid and frontal bones at positive PC scores. Representatives of Scombridae span the entire range of this PC. PC3 accounts for 6.3% of total shape variation and appears to be correlated with relative orbit size, ranging from large orbits seen in Caristiidae at negative PC values to smaller orbits at positive values. The first six PCs cumulatively account for 76% of total shape disparity, revealing that the majority of shape disparity in this data set is concentrated in a comparatively small number of axes of variation. Phylogenetic signal was significant but low across the whole neurocranium (K_{mult} = 0.27, P = 0.001).

Allometry is significantly correlated with neurocranium shape, but with a small effect size, both in raw shape data (R^2 = 0.06, Z = 2.57, P = 0.002) and after accounting for phylogeny (R^2 = 0.04, Z = 3.02, P = 0.003), suggesting that size has little influence on shape across the clade.

Cluster analysis

An examination of the morphospace occupancy density of PCs 1 and 2 suggests several regions of high occupancy (Figure 3). The cluster analysis performed on the shape data revealed three major clusters that broadly aligned with these regions, corresponding to three distinct morphotypes: morphotype 1 ("*Brama*"-type), with a shortened ethmoid region and tall supraoccipital crest; morphotype 2 ("*Gempylus*"-type), with elongate ethmoid region and small/no supraoccipital crest; and morphotype 3 ("*Scomber*"-type), intermediate in shape between morphotypes 1 and 2. Examining this plot also reveals some apparent convergence on these clusters. This is especially obvious at the boundary between morphotype 1 and morphotype 3, with members of Nomeidae, Ariommatidae, Scombridae, Bramidae, and Stromateidae all spanning this region. Mean phenotypic convergence within each clade is high (morphotype 1: C_1 = 0.666, C_3 = 0.309, C_4 = 0.008; morphotype 2: C_1 = 0.481, C_3 = 0.217, C_4 = 0.005; morphotype 3: C_1 = 0.462, C_3 = 0.227, C_4 = 0.005), and all were significantly different (P < 0.01) from the null expectation of evolutionary simulations (Figure 3; supplementary Table S6).

Modularity and integration

High integration of the neurocranium is supported by the results of the *compare.CR* analysis (Supplementary Table S3), with the strongest support for the four-module hypothesis in both raw shape (CR = 0.89, P = 0.001) and after accounting for phylogeny (CR = 0.73, P = 0.001; Figure 4, Supplementary Tables S2 and S3). This hypothesis groups are as follows: ethmoid, vomer, lateral ethmoid, and frontal into the *anterior neurocranium*; the parietal, supraoccipital, exoccipital, and basioccipital into the *occipital region*; epiotic, pterotic, intercalar, sphenotic, and prootic into the *otic region*; and the parasphenoid, pterosphenoid, and basisphenoid into the *sphenoid region*.

Ecology

Neurocranium shape was weakly correlated with habitat depth (Z = 2.49, P = 0.003, Figure 5A), but was non-significant when phylogeny was accounted for (Z = 0.63, P = 0.269). Pairwise comparison of depth categories revealed only marginally significant difference in the morphological disparity between the shallow and intermediate groups, but not between the shallow and deep groups (Supplementary Table S5), although the deep category had the highest disparity overall (deep = 0.0227, intermediate = 0.0221, shallow = 0.0173). Shape was found to be significantly correlated with fineness ratio (raw shape data: Z = 4.61, P = 0.001; phylogenetically informed: Z = 4.95, P = 0.001; Figure 5B), with long,

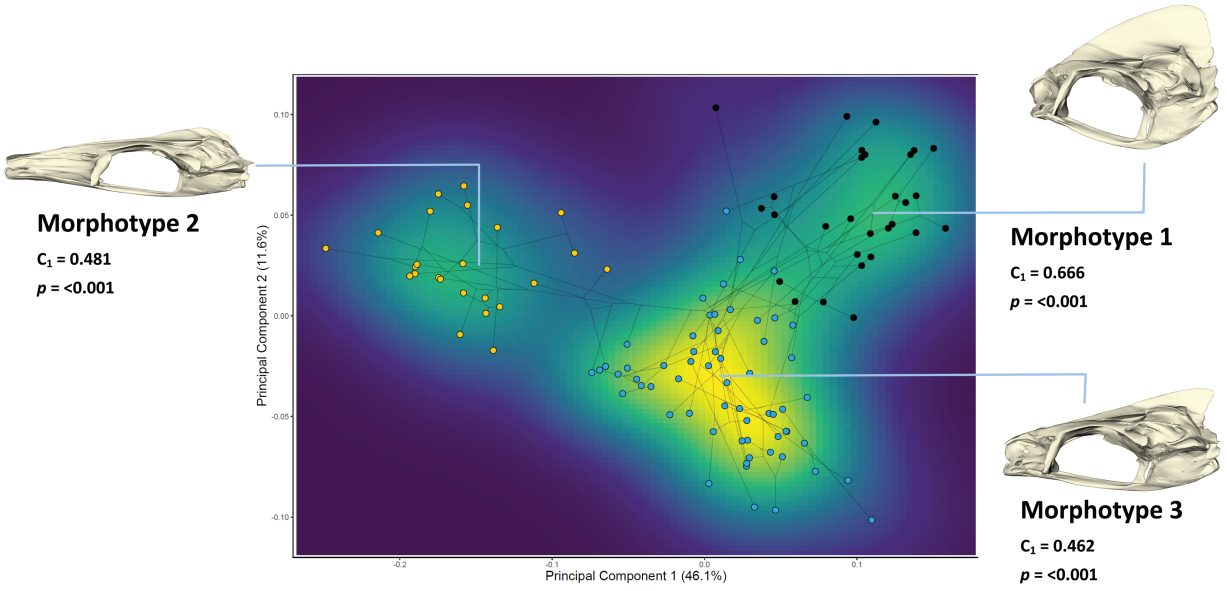

Figure 3. Heatmap showing occupancy density of PCs 1 and 2, with results of cluster analysis of neurocranium morphotypes. Points are colored according to the morphotype identified from cluster analysis. Meshes represent the mean neurocranium shape for each morphotype. Mean phenotypic convergence within each cluster (C_1) is shown with each mean shape, along with the associated p-value from 100 evolutionary simulations.

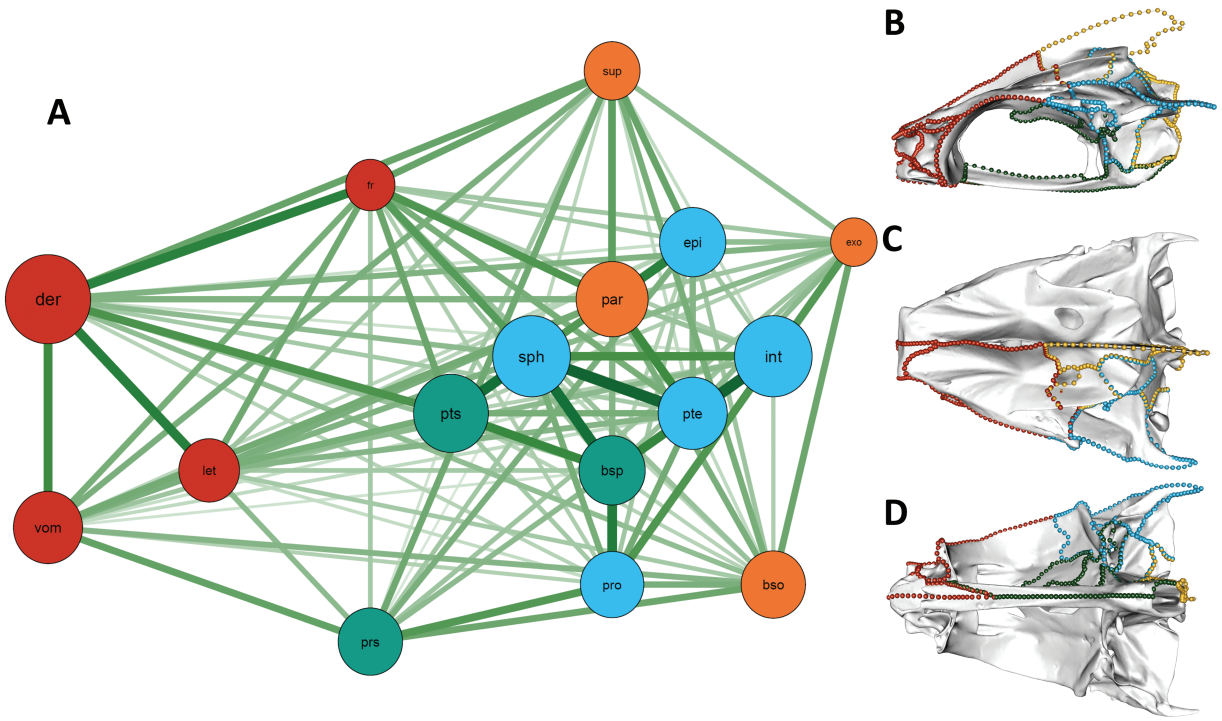

Figure 4. Results of modularity analyses. Network plot (A) shows the relative covariance within (circle size) and between (line thickness) skull elements, with each element colored according to best-supported module. Meshes show left lateral (B), dorsal (C) and ventral (D) views of neurocranium with landmarks colored according to module, as per network plot. Abbreviations are **der**: ethmoid, **let**: lateral ethmoid, **fr**: frontal, **sup**: supraoccipital, **exo**: exoccipital, **epi**: epiotic, **par**: parietal, **sph**: sphenotic, **int**: intercalar, **pte**: pterotic, **bsp**: basisphenoid, **pts**: pterosphenoid, **bso**: basioccipital, **pro**: prootic, **prs**: parasphenoid, **vom**: vomer.

shallow neurocrania being associated with elongate body shapes, and short, deep neurocrania associating with shorter body shapes. There appears to be a general trend in decreasing fineness ratio along PC1, with high fineness ratio values at negative PC scores and low values at positive PC scores (Figure 5B). As with depth, dietary categories were significant but with a small effect size in raw shape data (Z = 2.25, P = 0.012; Figure 5C), but nonsignificant after accounting for phylogeny (Z = 1.58, P = 0.07).

Evolutionary modeling

The BayesTraits analysis returned the strongest support for a single-rate OU evolution model for the whole neurocranium (Supplementary Figure S3). A single-rate OU model was also best-supported for each individual module, for both globally and locally aligned data sets. These results suggest that the pelagiarian neurocranium has undergone consistent rates in shape evolution with little major variation through time but that its shape tends to evolve toward a selective optimum. Evolutionary rate (σ^2_{mult}) across Pelagiaria was not found to be significantly different between the four modules for raw shape (observed rate ratio = 1.96, P = 0.316) or after accounting for phylogeny (observed rate ratio = 1.80, P = 1; Supplementary Table S4).

Discussion

Our results show that the shape disparity of the neurocranium in Pelagiaria is concentrated along relatively few axes of variation, with almost half of total intraspecific variation describing transitions from long and shallow to short and deep forms along PC1 (Figure 2). Body shape in Pelagiaria has been shown to be highly disparate, spanning the elongation continuum of teleosts (Collar *et al.*, 2022), and the strong correlation of neurocranium shape with body elongation further implies that neurocranium shape is highly disparate in this clade. Correlation of 3D skull shape and body elongation supports findings by Claverie and Wainwright (2014) in reef fishes, Gilbert *et al.* (2021) in Bramidae, Collar *et al.* (2022) in Pelagiaria, and Burns *et al.* (2023) in characiforms. The clustering of taxa within morphospace suggests that, although showing high shape disparity overall, there is a tendency for the neurocranium to evolve toward a small range of morphotypes. This is supported by significant and high levels of phenotypic convergence within clusters. The neurocranium plays an important role in structuring and streamlining the head and anterior body, and it is likely that evolutionary integration between body shape and neurocranium, and within the neurocranium itself, is due to the coordination of evolution and development among these elements.

Phenotypic integration is expected to play an important role in the evolution and development of complex structures such as the vertebrate skull because it allows coordinated responses to selection across multiple regions and elements. This in turn can be manifested in patterns of evolutionary integration across clades (Clune *et al.*, 2013; Goswami *et al.*, 2014; Hedrick *et al.*, 2020; Klingenberg, 2008; 2014). Several recent studies have used a geometric morphometric approach to assess phenotypic and evolutionary integration across a range of tetrapod taxa including caecilians (Bardua *et al.*, 2019), birds (Felice & Goswami, 2017; Navalón *et al.*, 2018), archosaurs (Felice *et al.*, 2019, 2021; Knapp *et al.*, 2021), mammals (Bibi & Tyler, 2022; Goswami & Polly, 2010; Hanot *et al.*, 2021; Menegaz & Ravosa, 2017; Randau

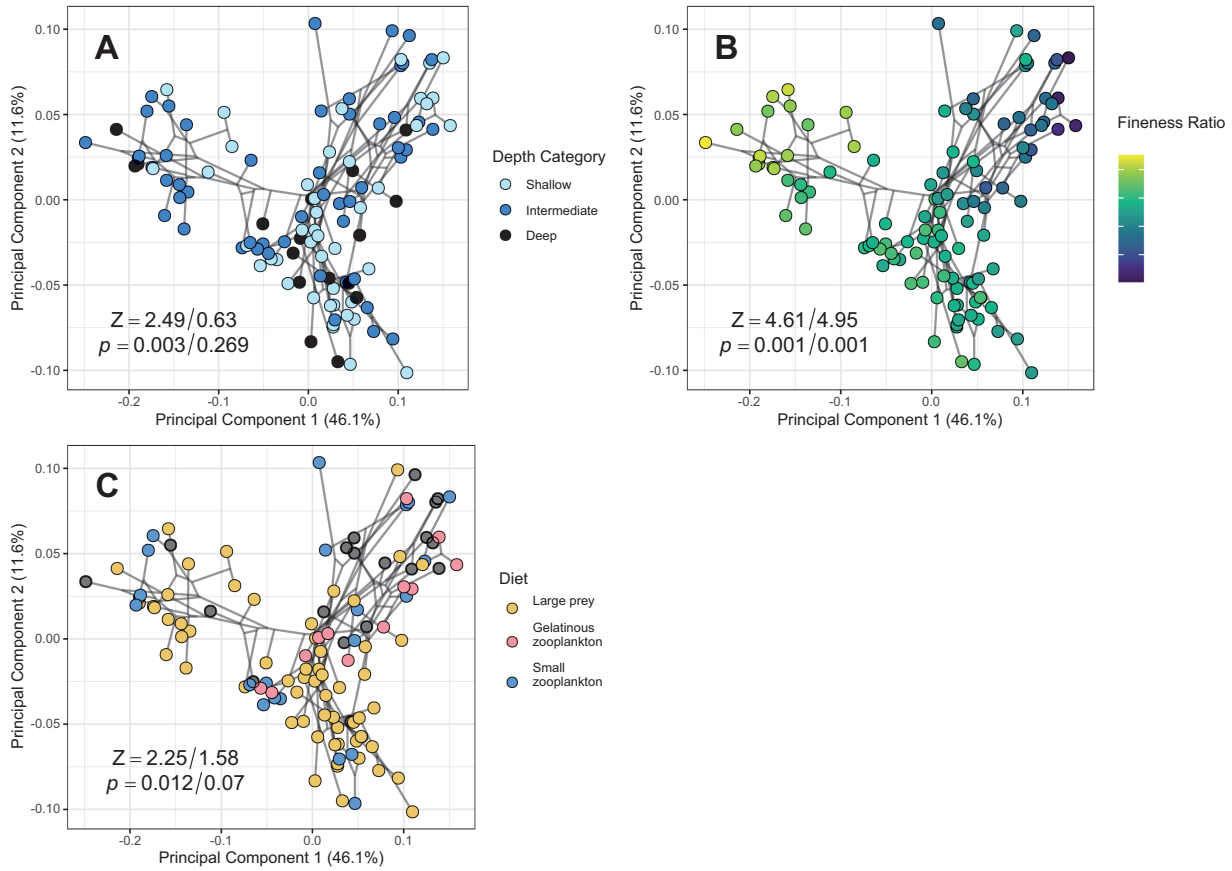

Figure 5. Phylomorphospace of neurocranium shape with specimens colored by (A) habitat depth, (B) fineness ratio, and (C) diet. MANOVA *Z* scores and *P*-values are shown on each plot, with results for raw shape data and phylogenetically informed analyses presented to the left and right of the slashes, respectively.

& Goswami, 2018), and squamates (Watanabe *et al.*, 2019), and have demonstrated conservation of patterns of integration from the phenotypic to evolutionary level. These studies tend to support more modular patterns across the tetrapod skull than our analyses found in the neurocranium of Pelagiaria, although we only interrogate evolutionary modularity here. The teleost neurocranium does not encompass elements involved in feeding that are partially or fully fused in the tetrapod skull (i.e., maxilla, premaxilla, quadrate, etc.). Evolutionary integration between the neurocranium and splanchnocranial elements of teleosts might be expected to be relaxed due to the diverse feeding strategies of teleosts (Collar *et al.*, 2014; Gibb *et al.*, 2015). In contrast, integration within the oral and pharangeal jaws of teleosts has been shown to be high in a number of recent studies (Conith & Albertson, 2021; Conith *et al.*, 2020; Jamniczky *et al.*, 2014; Larouche *et al.*, 2022). This is likely to be due to the complex linkages between the elements of the oral jaws (Westneat, 1990, 2004) and the importance of maintaining a functional relationship between the oral and pharangeal jaws (Larouche *et al.*, 2022). Nonetheless, when comparing a range of modularity hypotheses, our results support higher integration (i.e., fewer modules) compared with the neurocranium region of the tetrapod skull using equivalent methods, despite incorporating a higher number of elements overall. Incorporating elements of the oral jaws and suspensorium will allow us to make a more direct comparison to the tetrapod skull and clarify how modular the teleost skull is compared with tetrapods. A recent study found high evolutionary integration in the neurocranium of carangiform fishes, but linked this to the inclusion of Pleuronectiformes (flatfishes) in the data set, concluding that the migration of an eye across the sagittal plane of the neurocranium during ontogeny and the resulting directional asymmetry of the neurocranium in this clade was responsible for its high integration (Evans *et al.*, 2021). Despite using different landmarking schemes, it is notable that our data set also shows relatively high integration in the neurocranium even in the absence of a morphological feature this extreme. Both results support that elements of the neurocranium evolve in a highly integrated manner, and future work incorporating intraspecific data is necessary to establish whether this evolutionary integration is caused by close developmental, genetic, or functional associations of these elements.

The significant but relatively weak phylogenetic signal (K_{mult} = 0.27) recovered from neurocranium shape data suggests a substantial degree of phenotypic convergence within the data set. This is supported by the presence of three distinct clusters within the morphospace (Figure 3), suggesting that neurocranium shape in Pelagiaria tends to evolve within these somewhat restricted regions of the available morphospace. Gempylidae and Trichiuridae are the only families found in the Morphotype 2 group, but Morphotypes 1 and 3 are populated by taxa from numerous families, and crossing-over between these morphological groups is apparent within Nomeidae, Ariommatidae, Scombridae, Bramidae, and Stromateidae. The results of the phenotypic convergence analysis reveal that convergence within each cluster

is statistically significant and high in each case, showing an average phenotypic convergence of 67% in Morphogroup 1, 48% in Morphogroup 2, and 46% in Morphogroup 3 (Figure 3). It appears that the evolution of certain neurocranium shapes is favored, with lineages repeatedly evolving toward a restricted range of shape optima, and leaving some regions of morphospace entirely unoccupied (Supplementary Figure S4). Single-rate OU evolutionary models describe situations where traits are attracted to a selective optimum. The identification of three clusters within the shape data in our study, coupled with strong phenotypic convergence, suggests the evolution of multiple adaptive peaks, which is seemingly at odds with support for evolution toward a single optimum. Current OU models in BayesTraits or other existing software, however, cannot at present account for multiple adaptive peaks in multivariate date. The lack of substantial difference between morphological disparity of different depth groups in Pelagiaria contrasts with one previous study that showed the deep ocean to be a hotbed of body shape evolution in teleosts (Martinez *et al.*, 2021). It does not therefore seem that adaptation to different depth zones has notably influenced neurocranial or body shape disparity in this clade, but it is worth noting that this previous study was based on body shape disparity across a much wider range of taxa. The origination of distinctive crown pelagiarian lineages has been placed near the K/Pg boundary by molecular data (Friedman *et al.*, 2019), and distinctive family-level morphologies are known from Eocene fossils from several localities (Beckett *et al.*, 2018a, b; Friedman *et al.*, 2016), suggesting that morphological disparity was established early in clade diversification. An early burst model may therefore be expected to be supported in Pelagiaria, but this was not found in our study. Incorporating fossils may affect the best-supported evolutionary model, but the scarcity of well-preserved, 3D neurocranium fossils presently prevents this.

The role of the neurocranium both as a protective structure for the brain and sensory organs and as a rigid foundation for the kinetic elements of the skull likely plays an important role in shaping its morphological evolution. The pelagiarian neurocranium does not have an obvious direct mechanical function in the way that, for example, the mandible does (Deakin *et al.*, 2022), and so it is difficult to ascribe an adaptive optimum to any of these shapes based on measurable performance. The neurocranium has an important role in anchoring the postcranial epaxial muscles, which provide the necessary force to power suction feeding in some teleosts (Camp & Brainerd, 2014; Camp *et al.*, 2015). The strong correlation we found between neurocranium shape and body elongation in Pelagiaria highlights its importance in providing structural support and shaping the anterior body, and it is possible that taller occipital crests typically found in deeper skulls at positive values along PC1 (Figures 2 and 3) act as structural support for epaxial muscles at their connection with the dorsal surface of the neurocranium. Elongation of the anterior neurocranium may have evolved in Trichiuridae and Gempylidae to accommodate longer oral jaws, but this does not seem to be the case for the long-jawed Chiasmodontidae, which are placed midway along PC1 (Figure 2) due to their shortened anterior neurocranium. It is likely that this family accommodates its elongated oral jaws by instead evolving a posteriorly oriented quadrato-mandibular joint. As in other vertebrates, brain development may also influence neurocranium integration in some regions of the pelagiarian neurocranium (Evans *et al.*, 2017a; Hu & Marcucio, 2009; Northcutt & Kaas, 1995). This may account for the high integration and seemingly low disparity of the posterior neurocranium (sphenotic, otic, and occipital) when compared with the anterior neurocranium (Figures 2 and 3). The significant but comparatively weak correlations between neurocranium shape and both diet and depth categories, which disappear after accounting for phylogeny, suggest that these factors are unlikely to play a major role in shaping its morphological evolution. The need for the suspensorium and upper jaw to articulate at several points on the ventral and lateral parts of the neurocranium is likely to place some limits on the relative positions of these contact points to allow for efficient and combined movement of linked kinetic elements (Westneat, 2004). This in turn may depend on the shape and relative position of the elements themselves (Hu *et al.*, 2017). A recently published study incorporating kinetic skull elements suggested that modularity may influence morphological divergence in complex feeding structures in labrid fishes (wrasses) (Larouche *et al.*, 2022). Wrasses have evolved a diverse range of feeding strategies, which are likely to have been driven by the dietary diversity of their reef and shallow-water habitats. Although the open ocean is known to be a complex habitat that promotes phenotypic diversity (Friedman *et al.*, 2019; Martinez *et al.*, 2021), pelagiarian taxa do not exhibit certain feeding modes important in wrasses (e.g., grinding and crushing corals, hard-shelled invertebrates, etc.). Consequently, this may influence the evolutionary modularity of the kinetic skull elements in this clade because there is no requirement to evolve crushing jaws and dentition. Incorporating additional skull elements into this data set will thus let us investigate modularity across the pelagiarian skull and more fully compare across teleost clades.

Supplementary material

Supplementary material is available online at *Evolution* (https://academic.oup.com/evolut/qpad056).

Data availability

All scans are available as freely downloadable digital meshes from www.phenome10k.org. Primary CT data will be made available from www.morphosource.org.

Author contributions

A.K., G.R.L., M.F., and Z.J. conceived the study. A.K., G.R.L., K.E., M.F., H.T.B., and Z.J. collected and processed scan data. A.K. landmarked scan data. A.K. and A.G. analyzed data. All authors contributed to writing of the manuscript.

Conflict of interest: The authors declare no conflict of interest.

Acknowledgments

For access to specimens, we are grateful to James Maclaine, Ollie Crimmen, and Emma Bernard (NHMUK); Peter Rask Möller (NHMD); Peter Bartsch and Edda Assel (MfN); Philippe Béarez and Jonathan Pfliger (MNHN); and Amanda Hay (AMS). For assistance with scanning, we thank Vincent

Fernandez and Brett Clark (NHMUK), Kristen Mahlow (MfN), Marta Bellato (MNHN), and Jenny Gibson (Royal National Orthopaedic Hospital NHS Trust). We also thank current and past members of the Goswami Lab at the Natural History Museum, London, for valuable feedback and discussion, and two anonymous reviewers whose thoughtful comments and suggestions helped greatly improve our original manuscript. This study includes data produced in the CTEES facility at University of Michigan, supported by the Department of Earth and Environmental Sciences and College of Literature, Science, and the Arts, and from the Department of Earth Sciences, University of Oxford, Oxford, UK. This study was funded by a Leverhulme Trust grant, no. RPG-2019-113.

References

Adams, D. C., & Otárola-Castillo, E. (2013). Geomorph: An R package for the collection and analysis of geometric morphometric shape data. *Methods in Ecology and Evolution*, 4(4), 393–399. https://doi.org/10.1111/2041-210x.12035

Adams, D. C. (2016). Evaluating modularity in morphometric data: Challenges with the RV coefficient and a new test measure. *Methods in Ecology and Evolution*, 7(5), 565–572. https://doi.org/10.1111/2041-210x.12511

Arbour, J. H., Curtis, A. A., & Santana, S. E. (2021). Sensory adaptations reshaped intrinsic factors underlying morphological diversification in bats. *BMC Biology*, 19(1), 1–13.

Arcila, D., Hughes, L. C., Melélendez-Vazquez, F., Baldwin, C. C., White, W. T., Carpenter, K. E., Williams, J. T., Santos, M. D., Pogonoski, J. J., Miya, M., Orti, G., & Bentacur-R, R. (2021). Testing the utility of alternative metrics of branch support to address the ancient evolutionary radiation of tunas, stromateoids and allies (Teleostei: Pelagiaria). *Systematic Biology*, 70(6), 1123–1144. https://doi.org/10.1093/sysbio/syab018

Bardua, C., Wilkinson, M., Gower, D. J., Sherratt, E., & Goswami, A. (2019). Morphological evolution and modularity of the caecilian skull. *BMC Evolutionary Biology*, 19, 1–24. https://doi.org/10.1186/s12862-018-1342-7

Beckett, H. T., & Friedman, M. (2016). The one that got away from Smith Woodward: Cranial anatomy of Micrornatus (Acanthomorpha: Scombridae) revealed using computed microtomography. *Geological Society, London, Special Publications*, 430, 337–353.

Beckett, H. T., Giles, S., Johanson, Z., & Friedman, M. (2018a). Data from: Morphology and phylogenetic relationships of fossil snake mackerels and cutlassfishes (Trichiuroidea) from the Eocene (Ypresian) London Clay Formation. *Dryad Digital Repository*, 4(4), 1–27. https://doi.org/10.5061/dryad.7722q

Beckett, H. T., Giles, S., Johanson, Z., & Friedman, M. (2018b). Morphology and phylogenetic relationships of fossil snake mackerels and cutlassfishes (Trichiuroidea) from the Eocene (Ypresian) London Clay formation. *Papers in Palaeontology*, 4(4), 1–27. https://doi.org/10.1002/spp2.1221

Betancur-R, R., Wiley, E. O., Arratia, G., Acero, A., Bailly, N., Miya, M., Lecointre, G., & Ortí, G. (2017). Phylogenetic classification of bony fishes. *BMC Evolutionary Biology*, 17(1), 162. https://doi.org/10.1186/s12862-017-0958-3

Bibi, F., & Tyler, J. (2022). Evolution of the bovid cranium: Morphological diversification under allometric constraint. *Communications Biology*, 5(1), 1–12.

Black, C. R., & Armbruster, J. W. (2022). Evolutionary integration and modularity in the diversity of the suckermouth armoured catfishes. *Royal Society Open Science*, 9(11), 220713.

Burns, M. D., Collyer, M. L., & Sidlauskas, B. L. (2023). Simultaneous integration and modularity underlie the exceptional body shape diversification of characiform fishes. *Evolution*, 77(3), 746–762. https://doi.org/10.1093/evolut/qpac070

Camp, A. L., & Brainerd, E. L. (2014). Role of axial muscles in powering mouth expansion during suction feeding in largemouth bass (*Micropterus salmoides*). *Journal of Experimental Biology*, 217, 1333–1345. https://doi.org/10.1242/jeb.095810

Camp, A. L., Roberts, T. J., & Brainerd, E. L. (2015). Swimming muscles power suction feeding in largemouth bass. *Proceedings of the National Academy of Sciences*, 112(28), 8690–8695. https://doi.org/10.1073/pnas.1508055112

Cardini, A. (2016). Left, right or both? Estimating and improving accuracy of one-side-only geometric morphometric analyses of cranial variation. *Journal of Zoological Systematics and Evolutionary Research*, 55, 1–10. https://doi.org/10.1111/jzs.12144

Claverie, T., & Wainwright, P. C. (2014). A morphospace for reef fishes: Elongation is the dominant axis of body shape evolution. *PLoS One*, 9(11), e112732. https://doi.org/10.1371/journal.pone.0112732

Clune, J., Mouret, J. B., & Lipson, H. (2013). The evolutionary origins of modularity. *Proceedings of the Royal Society of London, Series B*, 280(1755), 20122863. https://doi.org/10.1098/rspb.2012.2863

Collar, D. C., Wainwright, P. C., Alfaro, M. E., Revell, L. J., & Mehta, R. S. (2014). Biting disrupts integration to spur skull evolution in eels. *Nature Communications*, 5(1), 1–9.

Collar, D. C., Tremaine, S., Harrington, R. C., Beckett, H. T., & Friedman, M. (2022). Mosaic adaptive peak shifts underlie body shape diversification in pelagiarian fishes (Acanthomorpha: Percomorpha). *Biological Journal of the Linnean Society*, 13(2), 324–340. https://doi.org/10.1093/biolinnean/blac096

Conith, A. J., Kidd, M. R., Kocher, T. D., & Albertson, R. C. (2020). Ecomorphological divergence and habitat lability in the context of robust patterns of modularity in the cichlid feeding apparatus. *BMC Evolutionary Biology*, 20(1), 1–20.

Conith, A. J., & Albertson, R. C. (2021). The cichlid oral and pharyngeal jaws are evolutionarily and genetically coupled. *Nature Communications*, 12(1), 1–11.

Deakin, W. J., Anderson, P. S. L., den Boer, W., Smith, T. J., Hill, J. J., Rücklin, M., Donoghue, P. C. J., & Rayfield, E. J. (2022). Increasing morphological disparity and decreasing optimality for jaw speed and strength during the radiation of jawed vertebrates. *Science Advances*, 8, 1–12. https://doi.org/10.1126/sciadv.abl3644

Denton, J. S. S., & Adams, D. C. (2015). A new phylogenetic test for comparing multiple high-dimensional evolutionary rates suggest interplay of evolutionary rates and modularity in lanternfishes (Myctophiformes, Myctophidae). *Evolution*, 69(9), 2425–2440. https://doi.org/10.1111/evo.12743

Evans, K. M., Waltz, B. T., Tagliacollo, V. A., Sidlauskas, B. L., & Albert, J. S. (2017a). Fluctuations in evolutionary integration allow for big brains and disparate faces. *Scientific Reports*, 7, 40431. https://doi.org/10.1038/srep40431

Evans, K. M., Waltz, B., Tagliacollo, V., Chakrabarty, P., & Albert, J. S. (2017b). Why the short face? Developmental disintegration of the neurocranium drives convergent evolution in neotropical electric fishes. *Ecology and Evolution*, 7(6), 1783–1801. https://doi.org/10.1002/ece3.2704

Evans, K. M., Vidal-García, M., Tagliacollo, V. A., Taylor, S. J., & Fenolio, D. B. (2019). Bony patchwork: Mosaic patterns of evolution in the skull of electric fishes (Apteronotidae: Gymnotiformes). *Integrative and Comparative Biology*, 59(2), 420–431. https://doi.org/10.1093/icb/icz026

Evans, K. M., Larouche, O., Watson, S. -J., Farina, S., Habegger, M. L., & Friedman, M. (2021). Integration drives rapid phenotypic evolution in flatfishes. *Proceedings of the Royal Society of London, Series B*, 118(18), 1–10. https://doi.org/10.1073/pnas.2101330118

Evans, K. M., Larouche, O., West, J. L., Gartner, S. M., & Westneat, M. W. (2022). Burrowing constrains patterns of skull shape evolution in wrasses. *Evolution & Development*, 25(1), 73–84.

Fabre, A. -C., Bardua, C., Bon, M., Clavel, J., Felice, R. N., Streicher, J. W., Bonnel, J., Stanley, E. L., Blackburn, D. C., & Goswami, A. (2020). Metamorphosis shapes cranial diversity and rate of

evolution in salamanders. *Nature Ecology and Evolution*, 4(8), 1129–1140. https://doi.org/10.1038/s41559-020-1225-3

Felice, R. N., & Goswami, A. (2017). Developmental origins of mosaic evolution in the avian cranium. *Proceedings of the Royal Society of London, Series B*, 115(3) 555–560. https://doi.org/10.1073/pnas.1716437115

Felice, R. N., Watanabe, A., Cuff, A. R., Noirault, E., Pol, D., Witmer, L. M., Norell, M. A., O'Connor, P. M., & Goswami, A. (2019). Evolutionary integration and modularity in the archosaur cranium. *Integrative and Comparative Biology*, 59(2), 371–382. https://doi.org/10.1093/icb/icz052

Felice, R. N., Pol, D., & Goswami, A. (2021). Complex macroevolutionary dynamics underly the evolution of the crocodyliform skull. *Proceedings of the Royal Society of London, Series B*, 288, 20210919. https://doi.org/10.1098/rspb.2021.0919

Ferguson-Gow, H. (2021). *BTprocessR: A set of tools to help with the interpretation and analysis of the output of BayesTraits MCMC analyses*. R package version 0.0.1. https://rdrr.io/github/hferg/BTprocessR/

Friedman, M. (2009). Ecomorphological selectivity among marine teleost fishes during the end-Cretaceous extinction. *Proceedings of the Royal Society of London, Series B*, 106, 5218–5223.

Friedman, M., Beckett, H. T., Close, R. A., & Johanson, Z. (2016). The English Chalk and London clay: Two remarkable British bony fish Lagerstatten. *Geological Society, London, Special Publications*, 430, 165–200.

Friedman, M., Feilich, K. L., Beckett, H. T., Alfaro, M. E., Faircloth, B. C., Černý, D., Miya, M., Near, T. J., & Harrington, R. C. (2019). A phylogenomic framework for pelagiarian fishes (Acanthomorpha: Percomorpha) highlights mosaic radiation in the open ocean. *Proceedings of the Royal Society of London, Series B*, 286, 20191502. https://doi.org/10.1098/rspb.2019.1502

Friedman, S. T., Price, S. A., & Wainwright, P. C. (2021). The effect of locomotion mode on body shape evolution in teleost fishes. *Integrative Organismal Biology*, 3(1), obab016. https://doi.org/10.1093/iob/obab016

Froese, R., & Pauly, D. (Eds.). (2022). *FishBase, version (08/2022)*. World Wide Web Electronic Publication. www.fishbase.org.

Gibb, A. C., Staab, K., Moran, C., & Ferry, L. A. (2015). The teleost intramandibular joint: A mechanism that allows fish to obtain prey unavailable to suction feeders. *Integrative and Comparative Biology*, 55(1), 85–96. https://doi.org/10.1093/icb/icv042

Gilbert, M. C., Conith, A. J., Lerose, C. S., Moyer, J. K., Huskey, S. H., & Albertson, R. C. (2021). Extreme morphology, functional trade-offs, and evolutionary dynamics in a clade of open-ocean fishes. *Integrative Organismal Biology*, 3(1), 1–22. https://doi.org/10.1093/iob/obab003

Goswami, A., & Polly, P. D. (2010). The influence of modularity on cranial morphological disparity in carnivora and primates (Mammalia). *PLoS One*, 5(3), e9517–e9518. https://doi.org/10.1371/journal.pone.0009517

Goswami, A., Smaers, J. B., Soligo, C., & Polly, P. D. (2014). The macroevolutionary consequences of phenotypic integration: From development to deep time. *Philosophical Transactions of the Royal Society, Series B*, 369, 20130254. https://doi.org/10.1098/rstb.2013.0254

Goswami, A., Watanabe, A., Felice, R. N., Bardua, C., Fabre, A. C., & Polly, P. D. (2019). High-density morphometric analysis of shape and integration: The good, the bad, and the not-really-a-problem. *Integrative and Comparative Biology*, 59(3), 669–683. https://doi.org/10.1093/icb/icz120

Gregory, W. K. (1932). *Fish skulls: A study of the evolution of natural mechanisms* (Vol. XXIII). Philadelphia (PA): Transactions of the American Philosophical Society. Art. II.

Hanot, P., Bayarsaikhan, J., Guintard, C., Haruda, A., Mijiddorj, E., Schafberg, R., & Taylor, W. (2021). Cranial shape diversification in horses: Variation and covariation patterns under the impact of artificial selection. *BMC Ecology and Evolution*, 21(1), 1–19.

Hedrick B. P., Mutumi G. L., Munteanu V. D., Sadier A., Davies K. T., Rossiter S. J., Sears K. E., Dávalos L. M., & Dumont, E. (2020). Morphological diversification under high integration in a hyper diverse mammal clade. *Journal of Mammalian Evolution*, 27(3), 563–575.

Hu, D., & Marcucio, R. S. A. (2009). SHH-responsive signaling center in the forebrain regulates craniofacial morphogenesis via the facial ectoderm. *Development*, 136(1), 107–116. https://doi.org/10.1242/dev.026583

Hu, Y., Nelson-Maney, N., & Anderson, P. S. L. (2017). Common evolutionary trends underlie the four-bar linkage systems of sunfish and mantis shrimp. *Evolution*, 71(5), 1397–1405. https://doi.org/10.1111/evo.13208

Hughes, L. C., Orti, G., Huang, Y., Sun, Y., Baldwin, C. C., Thompson, A. W., Arcila, D., Betancur, R. R., Li, C., Becker, L., Bellora, N., Zhao, X., Li, X., Wang, M., Fang, C., Xie, B., Zhou, Z., Huang, H., Chen, S., ... Shi, Q. (2018). Comprehensive phylogeny of ray-finned fishes (Actinopterygii) based on transcriptomic and genomic data. *PNAS*, 155(24), 6249–6254. https://doi.org/10.1073/pnas.1719358115

Jamniczky, H. A., Harper, E. E., Garner, R., Cresko, W. A., Wainwright, P. C., Hallgrímsson, B., & Kimmel, C. B. (2014). Association between integration structure and functional evolution in the opercular four-bar apparatus of the threespine stickleback, *Gasterosteus aculeatus* (Pisces: Gasterosteidae). *Biological Journal of the Linnean Society*, 111(2), 375–390.

Jeena, N. S., Rahuman, S., Roul, S. K., Azeez, P. A., Vinothkumar, R., Manas, H. M., Nesnas, E. A., Rathinam, A. M. M., Surya, S., Rohit, P., Abdussamad, E. M. & Gopalakrishnan, A. (2022). Resolved and redeemed: a new fleck to the evolutionary divergence in the genus *Scomberomorus* Lacepède, 1801 (Scombridae) with cryptic speciation. *Frontiers in Marine Science*, 9, 888463. https://doi.org/10.3389/fmars.2022.888463

Klingenberg, C. P. (2008). Morphological integration and developmental modularity. *Annual Review of Ecology and Systematics*, 39, 115–132.

Klingenberg, C. P. (2014). Studying morphological integration and modularity at multiple levels: Concepts and analysis. *Philosophical Transactions of the Royal Society B*, 369, 20130249. https://doi.org/10.1098/rstb.2013.0249

Knapp, A., Knell, R. J. & Hone, D. W. E. (2021). Three-dimensional geometric morphometric analysis of the skull of *Protoceratops andrewsi* supports a socio-sexual signalling role for the ceratopsian frill. *Proceedings of the Royal Society B*. 288, 20202938. https://doi.org/10.1098/rspb.2020.2938

Larouche, O., Zelditch, M. L., & Cloutier, R. (2018). Modularity promotes morphological divergence in ray-finned fishes. *Scientific Reports*, 8, 72–78. https://doi.org/10.1038/s41598-018-25715-y

Larouche, O., Gartner, S. M., Westneat, M. W., & Evans, K. M. (2022). Mosaic evolution of the skull in labrid fishes involves differences in both tempo and mode of morphological change. *Systematic Biology*. syac061.https://doi.org/10.1093/sysbio/syac061

Lehoux, C., & Cloutier, R. (2015). Building blocks of a fish head: Developmental and variational modularity in a complex system. *Journal of Experimental Zoology. Part B. Molecular and Developmental Evolution*, 324(7), 614–628. https://doi.org/10.1002/jez.b.22639

Martinez, C. M., Friedman, S. T., Corn, K. A., Larouche, O., Price, S. A., & Wainwright, P. C. (2021). The deep sea is a hot spot of fish body shape evolution. *Ecology Letters*, 24(9), 1788–1799. https://doi.org/10.1111/ele.13785

Meade, A., & Pagel, M. (2014). *BayesTraitsV3*. http://www.evolution.reading.ac.uk/BayesTraitsV4.0.0/BayesTraitsV4.0.0.html

Menegaz, R. A., & Ravosa, M. J. (2017). Ontogenetic and functional modularity in the rodent mandible. *Zoology*, 124, 61–72. https://doi.org/10.1016/j.zool.2017.05.009

Mimics v. 21.0. *Materialise NV, Leuven, Belgium, 1992–2015*. https://www.materialise.com/en/healthcare/mimics-innovation-suite/mimics

Miya, M., Friedman, M., Satoh, T. P., Takeshima, H., Sado, T., Iwasaki, W., Yamanoue, Y., Nakatani, M., Mabuchi, K., Inoue, J. G., Poulsen, J. Y., Fukunaga, T., Sato, Y., & Nishida, M. (2013).

Evolutionary origin of the Scombridae (Tunas and Mackerels): Members of a Paleogene adaptive radiation with 14 other pelagic fish families. *PLoS One*, 8(9), e73535. https://doi.org/10.1371/journal.pone.0073535

Monsch, K. A., & Bannikov, A. F. (2011). New taxonomic synopses and revision of the scombroid fishes (Scombroidei, Perciformes), including billfishes, from the Cenozoic of territories of the former USSR. *Earth and Environmental Science Transactions of the Royal Society of Edinburgh*, 102(4), 253–300. https://doi.org/10.1017/s1755691011010085

Navalón, G., Bright, J. A., Marugán-Lóbon, J., & Rayfield, E. J. (2018). The evolutionary relationship among beak shape, mechanical advantage, and feeding ecology in modern birds. *Evolution*, 73(3), 422–435. https://doi.org/10.1111/evo.13655

Nelson, J. S. (2006). *Fishes of the world* (4th ed., p. 601). John Wiley & Sons.

Northcutt, R. G., & Kaas, J. H. (1995). The emergence and evolution of mammalian neocortex. *Trends in Neurosciences*, 18(9), 373–379. https://doi.org/10.1016/0166-2236(95)93932-n

Pastana, M. N. L., Johnson, G. D., & Datovo, A. (2021). Comprehensive phenotypic phylogenetic analysis supports the monophyly of stromateiform fishes (Teleostei: Percomorphacea). *Zoological Journal of the Linnean Society*, 195(3), 841–963. https://doi.org/10.1093/zoolinnean/zlab058

R Core Team. (2013). *R: A language and environment for statistical computing*. R Foundation for Statistical Computing. http://www.R-project.org/

Rabosky, D. L., Chang, J., Cowman, P. F., Sallan, L., Friedman, M., Kaschner, K., Garilao, C., Near, T. J., Coll, M., & Alfaro, M. E. (2018). An inverse latitudinal gradient in speciation rate for marine fishes. *Nature*, 559(7714), 392–395.

Randau, M., & Goswami, A. (2018). Shape covariation (or the lack thereof) between vertebrae and other skeletal traits in felids: The whole is not always greater than the sum of parts. *Evolutionary Biology*, 45(2), 196–210. https://doi.org/10.1007/s11692-017-9443-6

Rhoda, D., Polly, P. D., Raxworthy, C., & Segall, M. (2021). Morphological integration and modularity in the hyperkinetic feeding system of aquatic-foraging snakes. *Evolution*, 75(1), 56–72. https://doi.org/10.1111/evo.14130

Roberts, C. M., McClean, C. J., Veron, J. E. N., Hawkins, J. P., Allen, G. R., McAllister, D. E., Mittermeier, C. G., Schueler, F. W., Spalding, M., Wells, F., Vynne, C., & Werner, T. B. (2002). Marine biodiversity hotspots and conservation priorities for tropical reefs. *Science*, 295(5558), 1280–1284. https://doi.org/10.1126/science.1067728

Rohlf, F. J., & Slice, D. (1990). Extensions of the Procrustes method for the optimal superimposition of landmarks. *Systematic Zoology*, 39(1), 40–59. https://doi.org/10.2307/2992207

Schlager, S. (2017). Morpho and Rvcg—Shape Analysis in R. In Zheng, G., Li, S., & Szekely, G. (Eds.), *Statistical shape and deformation analysis* (pp. 217–256). Academic Press.

Schultze, H. -P., Arratia, G., & Wilson, M. V. H. (2008). Nomenclature and homologization of cranial bones in actinopterygians. *Mesozoic Fishes*, 4, 23–48.

Stayton, C. T. (2015). The definition, recognition, and interpretation of convergent evolution, and two new measures for quantifying and assessing the significance of convergence. *Evolution*, 69(8), 2140–2153. https://doi.org/10.1111/evo.12729

Stratovan Checkpoint v. 2020.10.13.0859. (2020). *Stratovan Corporation*. https://www.stratovan.com/products/checkpoint

Thomson, K. S. (1993). Segmentation, the adult skull and the problem of homology. In: Hanken, J., & Hall, B. K. (Eds.), *The skull, Volume 2, Patterns of structural and systematic diversity*. The University of Chicago Press.

Tibshirani, R., Walther, G., & Hastie, T. (2001). Estimating the number of clusters in a dataset via the gap statistic. *Journal of the Royal Statistical Society: Series B*, 63, 411–423.

Wagner, G. P., & Altenberg, L. (1996). Perspective: Complex adaptations and the evolution of evolvability. *Evolution*, 50(3), 967–976. https://doi.org/10.1111/j.1558-5646.1996.tb02339.x

Watanabe, A., Fabre, A. C., Felice, R. N., Maisano, J. A., Müller, J., Herrel, A., & Goswami, A. (2019). Ecomorphological diversification in squamates from conserved pattern of cranial integration. *Journal of the Royal Statistical Society: Series B*, 116(29), 14688–14697. https://doi.org/10.1073/pnas.1820967116

Westneat, M. W. (1990). Feeding mechanics of teleost fishes (Labridae; Perciformes): A test of four-bar linkage models. *Journal of Morphology*, 205(269), 269–295. https://doi.org/10.1002/jmor.1052050304

Westneat, M. W. (2004). Evolution of levers and linkages in the feeding mechanism of fishes. *Integrative and Comparative Biology*, 44(378), 378–389. https://doi.org/10.1093/icb/44.5.378

Zelditch, M. L., & Goswami, A. (2021). What does modularity mean? *Evolution and Development*, 23(5), 377–403. https://doi.org/10.1111/ede.12390